Recombination Radiation from Diamond

P. J. DEAN AND I. H. JONES
Wheatstone Laboratory, King's College, Strand, London, England
(Received 14 October 1963)

The spectrum of the recombination radiation from diamond has been measured over the photon energy range 4.9–5.5 eV at 90, 160, 207, and 320°K. At 90°K, recombination emission has been detected from ten samples out of a batch of fifteen single crystals, the majority of which were known to be relatively defect free. The persistent and usually dominant spectral features are interpretable in terms of exciton annihilation with the emission into the lattice of one or more phonons. The energies of the single phonons and the proposed classifications are 0.085 eV (transverse acoustical), 0.134 eV (longitudinal optical and acoustical), and 0.142 eV (transverse optical). The details of these intrinsic features of the emission are in good agreement with predictions obtained from a recent analysis of the edge absorption spectrum of diamond. Other recombination bands can be interpreted in terms of exciton annihilation with the emission of the transverse optical phonon, together with the simultaneous intervalley scattering of the electron by a longitudinal acoustical phonon which is produced during the recombination process. The assignment of the intervalley phonon energies is supported by an analysis of the band-broadening contribution to the temperature dependence of the indirect energy gap, in which intravalley scattering is also apparent. The magnitudes of the experimental intervalley phonon energies show that the conduction band minima of diamond are situated at about 95% of the distance from the center of the Brillouin zone to the zone boundary in the ⟨100⟩ directions. This result defines the wave vector of the three phonons quoted above. Recombination emission bands are also observed which appear respectively to involve at the low-energy extremities the simultaneous emission of two or three phonons of energy comparable to the Raman energy (0.165 eV). Two sets of sharp two-component extrinsic recombination bands are present. Each component of a given set is displaced by approximately the same energy below the low-energy thresholds of the intrinsic longitudinal acoustical (LA)+ longitudinal optical (LO) and transverse optical (TO) bands (displacement energies 0.056 and 0.009 eV). These bands are thought to arise from the recombination of excitons bound to certain impurity or defect sites. One system (0.056-eV binding energy) is tentatively associated with the acceptor center of semiconducting (type IIb) diamond, which is thought to be substitutional aluminium. The anticipated corresponding recombination bands occurring without the emission of a phonon have not been identified, however.

INTRODUCTION

THOSE features of the recombination radiation spectrum which persist in relatively perfect single-crystal specimens (intrinsic features) have been shown to provide detailed information about the band structure of semiconducting materials in the neighborhood of the valence-conduction-band energy gap.[1] Silicon,[1,2] germanium,[1,3] silicon carbide[4] and several III-V and II-VI compounds have been investigated. Information concerning the exciton structure and, for materials with an indirect absorption edge transition, the phonon spectrum has been obtained. The detailed structure of the intrinsic recombination radiation is closely related to fine structure observed in the intrinsic absorption edge spectrum.[5] This correspondence can provide a useful check on the experimental absorption spectra, since the recombination radiation structure takes the form of well-defined peaks at low temperatures, in contrast to the absorption spectra.[6]

Very narrow recombination radiation bands have been observed for several materials.[2,7,8] These bands are displaced in energy slightly below the main (broader) intrinsic bands and are attributed to exciton recombination at impurity centers. Extrinsic features of different origin have also been observed in germanium[3] and in gallium phosphide.[9]

Intrinsic recombination radiation is difficult to detect in large band-gap semiconductors with indirect absorption edge transitions, since single-crystal material becomes increasingly difficult to synthesize in pure form as the energy gap increases. Impure material usually contains many important recombination centers at which the gap energy is partially or completely degraded into relatively low-energy lattice vibrations. Diamond, which is one of the most difficult materials to synthesize even in relatively impure form,[10] generally contains at least one radiationless recombination center and also a radiative center which gives rise to a broad emission band of peak energy equal to about one-half of the indirect energy gap.[11]

The present measurements were performed on single-crystal specimens of naturally occurring diamond. Optical emission of quantum energy comparable to the indirect band gap was looked for in synthetic and

[1] J. R. Haynes, M. Lax, and W. F. Flood, Phys. Chem. Solids 8, 392 (1959).
[2] J. R. Haynes, Phys. Rev. Letters 4, 361 (1960).
[3] C. Benoit a la Guillaume, Phys. Chem. Solids 8, 150 (1959).
[4] W. J. Choyke and L. Patrick, Phys. Rev. 127, 1868 (1962).
[5] J. R. Haynes, M. Lax, and W. F. Flood, in *Proceedings of the International Conference on Semiconductor Physics 1960* (Czechoslavakian Academy of Sciences, Prague, 1961), p. 423.
[6] T. P. McLean, Progr. Semicond. 5, 53 (1960).
[7] M. I. Nathan and G. Burns, Phys. Rev. 129, 125 (1963).
[8] C. Benoit a la Guillaume and O. Parodi, in *Proceedings of the International Conference on Semiconductor Physics, 1960* (Czechoslovakian Academy of Sciences, Prague, 1961), p. 426.
[9] J. J. Hopfield, D. G. Thomas, and M. Gerschenzon, Phys. Rev. Letters 10, 162 (1963).
[10] C. M. Huggins and P. Cannon, Nature 194, 829 (1962).
[11] P. J. Dean and J. C. Male, Phys. Chem. Solids (to be published).

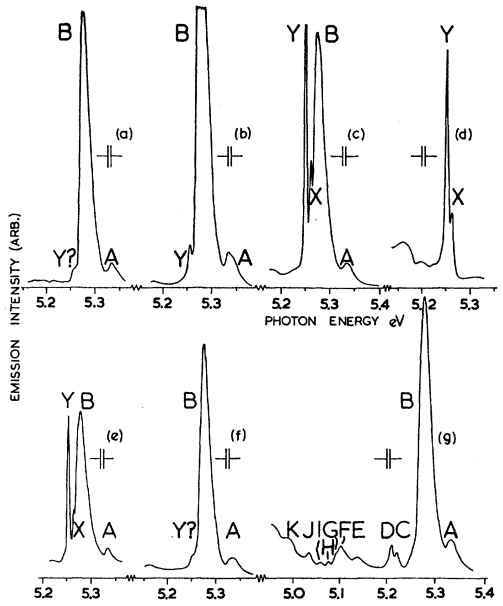

FIG. 1. Recombination radiation spectra from a selection of natural diamonds. (a) Specimen Co72 (type IIa) 70-keV, 220-μA electron beam; 0.0063-eV resolution; (b) specimen K80 (type IIa) 78-keV, 240-μA electron beam; 0.0063-eV resolution; (c) specimen X60 (intermediate type) 80-kV, 250-μA electron beam; 0.0063-eV resolution; (d) specimen WXR.1 (type I) 80-kV, 250-μA electron beam; 0.0063-eV resolution; (e) specimen C″116 (intermediate type) 80-kV, 220-μA electron beam; 0.0063-eV resolution; (f) specimen D10 (type IIa) 72-kV, 240-μA electron beam; 0.0063-eV resolution; (g) specimen E2 (type IIb) 30-kV, 220-μA electron beam; 0.0063-eV resolution. Ordinate—emission intensity (arbitrary); Abscissas—photon energy (eV).

synthetically doped specimens without success. Recombination radiation in diamond has been reported previously[12] for only one natural specimen excited by electroluminescence and measured at a single temperature (350–400°K), and with a relatively poor instrumental bandwidth (0.035 eV). This spectrum has been shown to be consistent with the edge absorption data.[13]

EXPERIMENTAL

The optical emission was stimulated by bombardment with an electron beam of energy between 10 and 80 keV. The beam current was varied between about 20 and 250 μA. Microscopic examination of the visible luminescence distribution showed that an area of 0.2 mm diam was luminescing when the electron beam was focused on to the specimen surface as sharply as possible. Calculations suggest that the local temperature rise produced in the most perfect specimens at an ambient temperature of 90°K was $\lesssim$5°K under the average conditions of excitation, but became more significant at the highest levels of input power. The specimens were mounted in Woods metal, with close contact to all faces other than the one under irradiation. The

[12] J. C. Male and J. P. Prior, Nature **186**, 1037 (1960).
[13] P. J. Dean and J. C. Male, Proc. Roy. Soc. (London) (to be published).

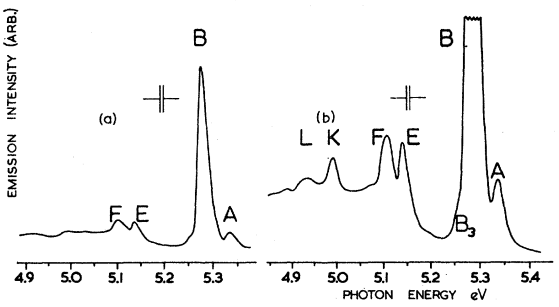

FIG. 2. Recombination radiation spectra from a natural diamond (type IIa, specimen DI). (a) 70-kV, 200-μA electron beam; 0.0063-eV resolution, gain 1; (b) 70-kV, 200-μA electron beam; 0.0063-eV resolution, gain 4; Ordinate—emission intensity (arbitrary); Abscissas—photon energy (eV).

mounted specimens were attached to the nose-piece of a metal Dewar arranged so that the electron beam was normally incident upon the specimen surface. The optical emission was viewed along a direction 45° to that of the electron beam. Initially a Hilger type-E484 spectrometer equipped with Kodak type-0-0a uv sensitized photographic plates was used to analyze the emission. Exposure times of $\sim$12 h were necessary with a spectral bandwidth of 0.011 eV and the recorded spectral intensities were distorted due to the approximately tenfold decrease in the quantum sensitivity of the photographic plates within the relevant energy range ($\sim$5.0–5.4 eV). The specimen surfaces sometimes became slightly pitted during the long exposures, presumably because of residual negative-ion bombardment. The pressure in the electron beam chamber was normally $<10^{-4}$ mm Hg.

Attempts to record the optical emission photoelectrically were initially frustrated by the poor stability of the electron beam. These difficulties were eventually overcome and the spectra were recorded using a Hilger type-E498 spectrometer converted to photoelectric detection with an EMI type-6256B quartz window photomultiplier. Practically noise-free pen-recorder traces of the spectra were obtained for the specimens

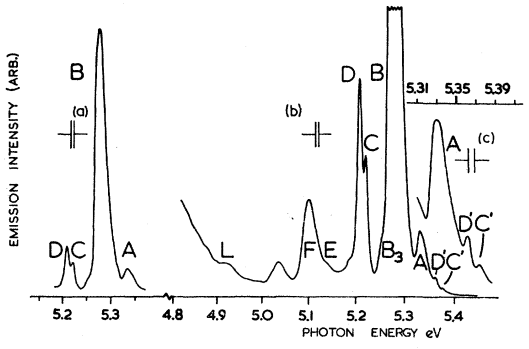

FIG. 3. Recombination radiation spectra from a natural diamond (type IIb, specimen A100). (a) 70-kV, 90-μA electron beam; 0.0063-eV resolution, gain 1; (b) 60-kV, 90-μA electron beam; 0.0063-eV resolution, gain 4.2; (c) 60-kV, 90-μA electron beam; 0.0063-eV resolution, gain 14; Ordinate—emission intensity (arbitrary); Abscissas—photon energy (eV).

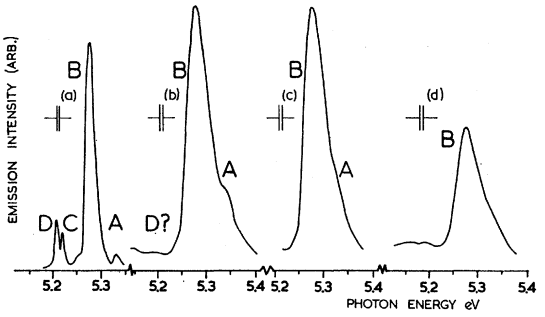

FIG. 4. Recombination radiation spectra from diamond at various specimen temperatures (type IIb, specimen A100). (a) 90°K; 80-kV, 220-μA electron beam, resolution 0.0045 eV, gain 1; (b) 160°K; 80-kV, 250-μA electron beam, resolution 0.0063 eV, gain 10; (c) 207°K; 80-kV, 250-μA electron beam, resolution 0.0063 eV, gain 13; (d) 320°K, 80-kV, 250-μA electron beam, resolution 0.0063 eV, gain 50; Ordinate—emission intensity (arbitrary); Abscissas—photon energy (eV).

which gave the strongest recombination emission signal, with a spectral bandwidth of 0.0063 eV and a scanning time of ~20 min. The energy scale of the recordings was determined using Hg and Cd emission lines of known energy.[14] The intensity of the main emission peak at the absorption edge (band B of Figs. 1–3 below) was only 0.1% of that of visible emission band for the specimen which gave the strongest edge band.

RESULTS AND DISCUSSION

A selection of the emission spectra obtained at 90°K is shown in Fig. 1. The optical absorption and electrical properties of the ten specimens for which well resolved spectra were obtained confirmed expectation that the strongest signal should be obtained from the most perfect specimens (in general those which would be definitely classified on the basis of their optical absorption spectra as type IIa or type IIb specimens). Figure 1 shows that the relatively broad bands A and B are the most persistent features of the spectra, particularly for the most perfect specimens. The sharp bands C and D are present only in the spectrum from the semiconducting (type IIb) specimen [Fig. 1(g)], which also contains a number of other sharp and broad bands at lower energies (bands E–K). The spectrum of another type-IIa specimen is shown in Fig. 2. Bands A and B are dominant, but bands C, D and X, Y are absent and the general shape of the spectrum below 5.2 eV is different from that of the $E2$ spectrum shown in Fig. 1. Bands E, F, and K are present in both spectra, however. Bands A, B, C, D, F, and L are plainly evident in the spectrum from a second type-IIb specimen (Fig. 3), but bands E and K are relatively weak and a strong band is present just below band F which is not present in Figs. 1 and 2. Figure 3 also shows two relatively sharp bands C' D' on the high-energy tail of band A.

Analysis of Intrinsic Features

Band B corresponds to the main feature in the spectrum recorded by Male and Prior.[12] There is a small shift in energy due to the ~300°K temperature difference between the measurements, and the band is appreciably broadened by increase in the crystal temperature (Fig. 4). Figure 4 also shows that bands C, D

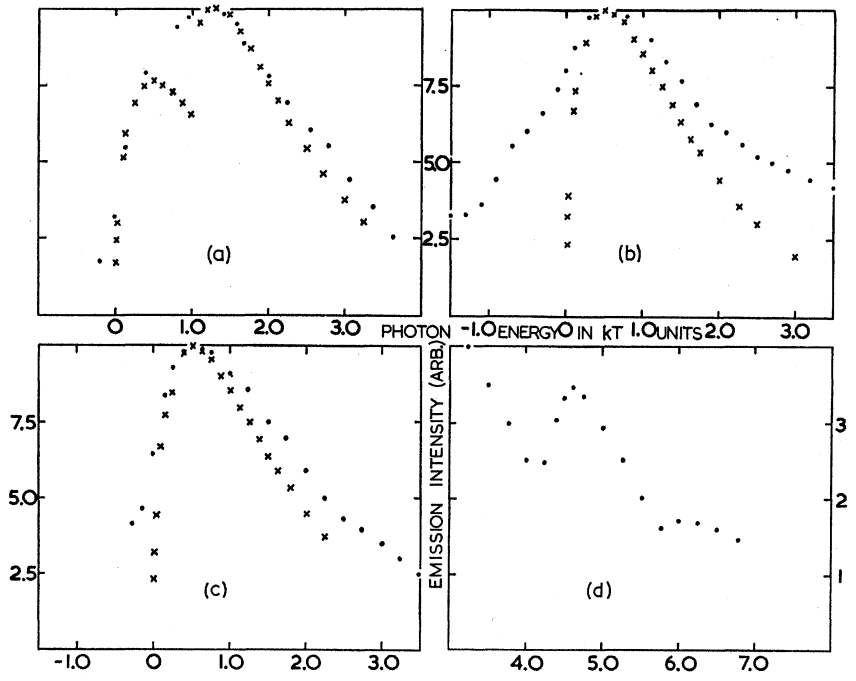

FIG. 5. Analysis of recombination radiation spectra (type IIb, specimen A100, 90°K). (a) Band B ●—experimental points, ×—Maxwell-Boltzmann components; (b) Band F ●—experimental points, ×—Maxwell-Boltzmann component; (c) Band A ●—experimental points, ×—Maxwell-Boltzmann component; (d) Bands C', D' ●—experimental points [continued from graph (c)]; Ordinate—emission intensity (arbitrary); Abscissas—photon energy (units of kT from M.B. thresholds).

[14] S. Zwerdling and J. P. Theriault, Spectrochi. Acta **17**, 819 (1961).

are very weak at temperatures $\gtrsim 160°K$. If, as previously suggested,[13] the intrinsic features of the recombination radiation are due to exciton recombinations, the low-energy threshold E_i of each recombination component should be given by

$$E_i = E_g - E_x - \hbar\omega_i, \quad (1)$$

where E_g is the indirect energy gap, E_x the exciton binding energy and $\hbar\omega_i$ the energy of one of the phonons which can satisfy the selection rules for the transition. Electron-hole recombination via the exciton state should be much more important than the recombination of free electrons and holes since $E_x \sim 10kT$ at 90°K and $\sim 3kT$ at 300°K.[5] The shape of each intrinsic recombination radiation component should be defined by the kinetic energy distribution of the excitons and should therefore be Maxwellian.

Figures 1, 2, and 3 show that band B is significantly broader than band A. Band B has been analyzed into two 90°K Maxwell-Boltzmann curves (assuming that the temperature of the directly stimulated region of the specimen was not significantly different from the bulk temperature), since two closely spaced phonon components are anticipated from the absorption edge data.[15] The magnitude of the component corresponding to the larger value of $\hbar\omega_i$ was made 11/7 the value of that of the second component,[15] and the relative positions of the two components was adjusted to obtain the best fit to the experimental recombination-emission curve [Fig. 5(a)]. The resulting values of E_i are 5.268 and 5.276 eV (components B_2 and B_1). Figure 5(a) shows that the agreement is good except for difference attributable to the experimental bandwidth and the comparatively large discrepancy just below the 5.276-eV threshold. This divergence may be due to the fact that this component probably represents two experimentally unresolved components [see Fig. 7(b)]. Band B can be approximately represented by a single Maxwell-Boltzmann component at higher temperatures, when the separation of the subcomponents becomes less than kT (Fig. 6). The high density of excitation and the decreased thermal conductivity of diamond at[16] 300°K resulted in a significant difference between the exciton distribution temperature and the ambient temperature ($\sim 25°K$). E_i decreases with increase in temperature [5.273 eV (single component fit), 5.270, 5.268, and 5.263 eV at 90, 160, 207, and 320°K], in good agreement with previous data on the temperature dependence of $E_g - E_x$.[13,15]

The fit of a single Maxwell-Boltzmann component to band A gives $E_i = 5.325$ eV. The experimental curve is significantly broader than the theoretical one on the high-energy side [Fig. 5(c)], possibly due to the presence of weak free-carrier recombination radiation associated with the band-B exciton components (calculated thresholds are 5.338 and 5.346 eV if[15] $E_x = 0.070$ eV, i.e., just above the band-A peak energy of 5.333 eV). $E_g - E_x$ is 5.410 ± 0.001 eV at 90°K.[13,15] The values of $\hbar\omega_i$ can therefore be found from Eq. (1) using the ex-

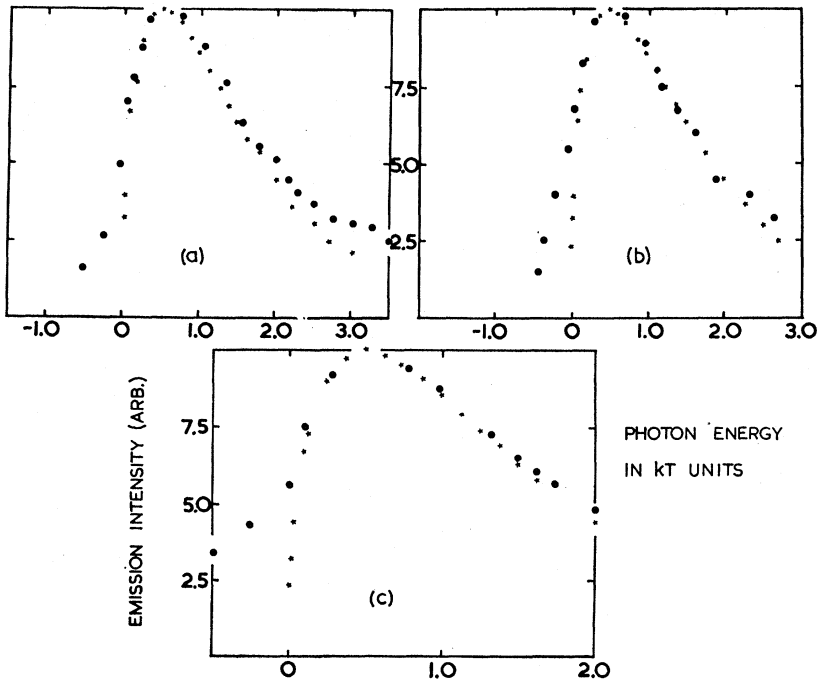

FIG. 6. Analysis of recombination spectra (type IIb, specimen A100, band B). (a) Dewar temperature $\sim 160°K$ ●—experimental points, ★—best fit with single Maxwell-Boltzmann components for $T = 160°K$; (b) Dewar temperature $\sim 200°K$ ●—experimental points, ★—best fit with single Maxwell-Boltzmann components for $T = 210°K$; (c) Dewar temperature $\sim 295°K$ ●—experimental points, ★—best fit with single Maxwell-Boltzmann components for $T = 320°K$; Ordinate—emission intensity (arbitrary); Abscissas—photon energy (units of kT from the M.B. threshold).

[15] C. D. Clark, P. J. Dean, and P. V. Harris, Proc. Roy. Soc. (London) (to be published).
[16] R. Berman, F. E. Simon, and J. Wilks, Nature **168**, 277 (1951).

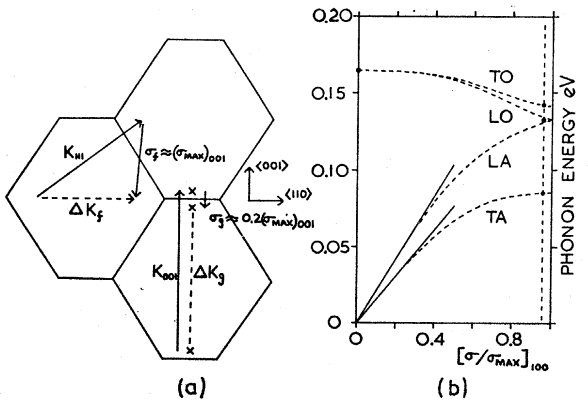

FIG. 7. (a) ⟨110⟩ plane cross section of adjacent Brillouin zones of diamond showing momentum conservation conditions for intervalley scattering [see D. Long, Phys. Rev. **120**, 2077 (1960)] [drawn for clarity assuming conduction band minima lie at $\sigma/\sigma_{max}=0.9$ instead of 0.95 as proposed in text and in Fig. 7(b)]. (b) Proposed lattice vibrational dispersion curve for diamond in the ⟨100⟩ direction constructed from the phonon energies which assist the indirect transitions; Ordinate—vibrational energy (eV); Abscissas—reduced wave vector $[\sigma/\sigma_{max}]_{\langle 100\rangle}$; ●—experimental points; straight lines—velocity of sound data.

perimental threshold energies giving

$$\hbar\omega_1=0.085\pm0.002 \text{ eV},$$
$$\hbar\omega_2=0.134\pm0.003 \text{ eV}, \quad (2)$$
$$\hbar\omega_3=0.142\pm0.003 \text{ eV}.$$

These energies are in good agreement with the values previously determined from absorption data.[15] The classification of these phonon components has already been discussed.[15] The ratio of the areas of bands B and A should be equal to the intensity ratio of the appropriate components in that part of the absorption edge spectrum for which phonons are emitted into the lattice [18:1 according to (15)]. Analysis of Figs. 1 to 3 gives the intensity ratio of bands B and A as ~20:1 so agreement is good.

The magnitude of bands A, B and $C+D$ was measured as a function of the electron-beam energy at constant electron current, and as a function of the electron current at constant energy. The results summarized in Table I are rather qualitative, since it was impossible to ensure exact positional and areal reproducibility of the irradiated region of the specimen, and it was not possible to follow either variation over more than a single decade of current or energy.

For a simple injecting contact on an insulator, the emission signal is expected to increase as a power of the injection current.[17] If defect trapping and recombination are important, however, the carrier lifetime may be dependent upon the injection level and the emission intensity may be a superlinear function of the current on a double-logarithmic plot. The rapid decrease in the intensity of the total recombination signal with increase in the specimen temperature (integrated signals at 200 and at 320°K were only ~18% and ~3% of the 90°K value, respectively, for specimen A100, and less for other specimens) suggests that trapping effects were significant during the present measurements. The attainment of a given level of trap saturation becomes increasingly difficult with increase in the temperature, presumably causing the observed temperature quenching of the intrinsic emission.

The observed variation of emission intensity of bands A and B with E_e probably arises from a rapid decrease in the density of trapping and recombination centers with increase in the penetration depth of the primary excitation.[11,18]

The half-height bandwidth Δ of band B increased by ~35% (i.e., an increase in effective temperature of ~30°K) as the current of a sharply focused 80-keV electron beam was increased from 25 to 200 μA, and a further increase in Δ of ~30% was observed between 200 and 250 μA. The calculated generation rate of secondary carriers under typical conditions of excitation is $\sim5\times10^{23}$ electrons cm^{-3} sec^{-1}. Using the free-carrier lifetime obtained from β-particle conduction counting experiments (unperturbed crystal value, the value presently appropriate is probably greater) the calculated injected carrier density is $\sim5\times10^{15}$ electrons cm^{-3}. This is comparable with the excess carrier density required to produce appreciable recombination radiation in other materials.[19]

Band F is similar in appearance to band B and Fig. 5(b) shows that its breadth is considerably greater than that of a single Maxwell-Boltzmann component. The value of E_i from the fitted curve gives $\hbar\omega=0.312$ eV, approximately equal to the sum of the Raman energy, $\hbar\omega_R=0.165$ eV, and $\hbar\omega_3$. The threshold of the experimental curve gives $\hbar\omega=0.324$ eV or 0.165+0.159 eV. Other types of combination are possible, involving two phonons both with finite wave vectors, and this may account for the width of the experimental curve.[13] The threshold of band L gives $\hbar\omega=0.500$ eV or about $3\hbar\omega_R$. The relative intensities of these multiphonon components are rather large compared with other materials[5] possibly because they are enhanced by the presence of suitable imperfections.[13] This assumption could also account for the observed specimen dependence of band

TABLE I. Dependence of band intensity on the electron beam current and energy. Specimen A100, 90°K.

Variable parameter	Band A	Band B	Band $C+D$
Electron-beam energy E_e (i.e., depth of penetration)	Intensity propl. $\exp(E_e)^{2.7}$	Intensity propl. $\exp(E_e)^{2.5}$	Intensity propl. E_e
Electron-beam current, I_e	Intensity propl. $\exp(I_e)$	Intensity propl. $\exp(I_e)$	Intensity propl. $\exp(I_e)$

[17] V. S. Vavilov, Usp. Fiz. Nauk **68**, 247 (1959) [English transl.: Soviet Phys.—Usp. **2**, 455 (1959)].

[18] J. E. Ralph, Ph.D. thesis, London, 1960 (unpublished).

[19] P. H. Brill and R. F. Schwarz, Phys. Rev. **112**, 330 (1958).

shape and intensity relative to band B in this region of the spectra.

The ratio of the probability of a transition involving n phonons to that involving one should be larger even in perfect diamond than in silicon by a factor of $\sim 11:1$ if the appropriate ground-state radii of the indirect exciton is used instead of the radii of the shallow impurity levels.[20] This suggests why bands involving multiphonon emission should be prominent for diamond, but does not explain the specimen dependence of intensity and shape for bands of different n observed here and in the edge excitation spectra for visible luminescence. The relative intensity of the emission and excitation bands also decrease much more slowly with increase in n above $n=2$ than predicted by the theory[20] in the absence of additional defects.

Intervalley Scattering

The experimental curves (Figs. 1–3) suggest the presence of a partially resolved component (B_3) at the low-energy threshold of band B. This is unlikely to be an artifact due to internal electric fields,[21] etc., since there is no trace of a similar feature at band A. When the B_2 and B_1 components are subtracted from band B, component B_3 has roughly the half-bandwidth expected for a 90°K exciton peak. The intensity of band B_3 is $\sim 35\%$ of that of band A, i.e., about 2% of band B. If B_3 is identified with a two-phonon exciton component involving $\hbar\omega_3$, by analogy with the silicon spectrum,[5] then the energy of the additional phonon $\hbar\omega_4$ is only 0.023 eV. Band B_3 is unlikely to be due to a single-phonon induced transition, since the resulting phonon energy is too large (0.165 eV, equal to $\hbar\omega_R$) and the band intensity is anomalously low for a transition involving a transverse optical phonon.[5]

The only likely explanation of the small magnitude of $\hbar\omega_4$ is that it is associated with intervalley scattering.[22] The conduction band minima in diamond are believed to lie near the boundary of the Brillouin zone in the ⟨100⟩ direction[15] and $\hbar\omega_4$ could cause intervalley scattering between conduction-band valleys on the same zone axis. This is the so-called g-scattering event shown in Fig. 7(a), which is forbidden for transverse acoustical (TA) phonons. From the linear portion of the longitudinal acoustical (LA) dispersion curve near $\sigma=0$, which is determined from the experimental velocity of sound measurements[23] [Fig. 7(b)], and the observed value of $\hbar\omega_4$, the position of the conduction band minima can be determined. The present result indicates that the minima are at about $0.05\ \sigma_{\max}$ from the ⟨100⟩ zone boundaries, as suggested previously.[15]

The f-scattering event involves the transfer of an electron from a given valley to one of the four others not on the same zone axis. Figure 7(a) shows that an LA phonon of energy close to that at $\sigma_{\max}$ ⟨100⟩ is required —i.e., close to the value of $\hbar\omega_2$ given in Eq. (2). The appropriate value of E_i should therefore be ~ 0.135 eV below the B_2 threshold—i.e., close to 5.133 eV. Band E may represent this process, but only in Fig. 2 is the magnitude and shape of this band of the expected order.[22] The specimen dependence of band E may be another manifestation of competing defect scattering mechanisms.

The dispersion curves of Fig. 7(b) have been drawn in accordance with the phonon energies of Eq. (2), the Raman energy, the velocity of sound measurements and the intervalley scattering data. The disagreement with the previously published dispersion curves[24] has been fully discussed elsewhere.[15]

Information concerning carrier scattering processes can also be obtained from the thermal broadening contribution to the temperature dependence of the energy gap,[25] $[dE_g/dT]_B$. The equation

$$d(E_g-E_x)/dT=[d(E_g-E_x)/dT]_B+[d(E_g-E_x)/dT]_D \quad (3)$$

can be used to calculate $[d(E_g-E_x)/dT]_B$ from the directly measured $d(E_g-E_x)/dT$[13,15] and the lattice dilation term $[d(E_g-E_x)/dT]_D$, which can be derived in turn from the experimental values of the volume expansion coefficient, α,[26] the compressibility, β,[27] and the pressure dependence of E_g-E_x, using equation

$$[d(E_g-E_x)/dT]_{P,D}=\frac{-\alpha}{\beta}[d(E_g-E_x)/dP]_T. \quad (4)$$

Neglecting the pressure and temperature dependence of E_x, these equations can be regarded to determine $[dE_g/dT]_B$. A provisional estimate of $[d(E_g-E_x)/dP]_T$ has been recently obtained by the present authors [$+5\times 10^{-7}$ eV $(\text{atm})^{-1}$]. The sign of this coefficient is contrary to expectation.[28] The calculated temperature dependences of $[d(E_g-E_x)/dT]_D$ and of $[d(E_g-E_x)/dT]_B$ are shown in Fig. 8(a). The rapid increase in $[d(E_g-E_x)/dT]_B$ between 180 and 350°K is presumably due to the increasing population of the lattice vibrational bands,[15] which is also reflected in the temperature dependence of the carrier mobility.[29]

The integrated change in (E_g-E_x) due to thermal broadening is plotted semilogarithmically against reciprocal temperature in Fig. 8(b). Five activation energies appear in the slope, the smallest of which is poorly substantiated since the curve was obtained by extrapolation for $10^3/T<12\,(°\text{K})^{-1}$. $\hbar\omega_\delta$ agrees in magnitude with $\hbar\omega_4$ above and $\hbar\omega_\alpha$ agrees with $\hbar\omega_2$ (approximately).

[20] J. R. Hardy, Proc. Phys. Soc. (London) **79**, 1154 (1962).
[21] D. Redfield, Phys. Rev. **130**, 914 (1963).
[22] W. P. Dumke, Phys. Rev. **118**, 938 (1960).
[23] H. J. McSkimin and W. L. Bond, Phys. Rev. **105**, 116 (1957).
[24] J. R. Hardy and S. D. Smith, Phil. Mag. **6**, 1163 (1961).
[25] M. L. Cohen, Phys. Rev. **128**, 131 (1962).
[26] S. I. Novikova, Fiz. Tverd. Tela **2**, 1617 (1960) [English transl.: Soviet Phys.—Solid State **2**, 1464 (1961)].
[27] P. W. Bridgman, *Physics of High Pressure* (G. Bell and Sons, London, 1931).
[28] W. Paul, J. Appl. Phys. Suppl. **32**, 2082 (1961).
[29] P. T. Wedepohl, Proc. Phys. Soc. (London) **70**, 177 (1957).

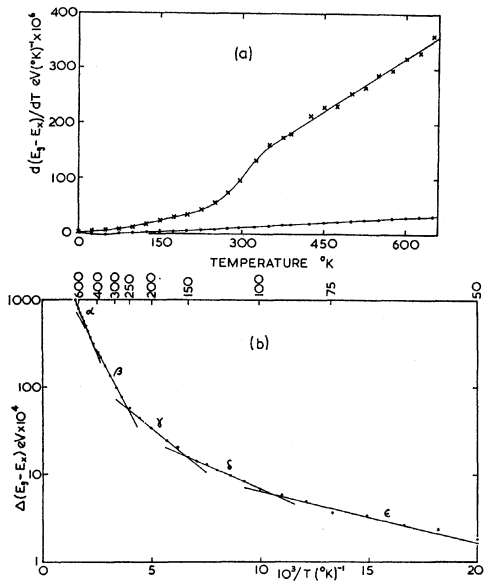

FIG. 8(b). Temperature derivative of (E_g-E_x) due to the electron-phonon interaction or "band broadening" (×—curve) and to lattice expansion (●—curve) plotted as a function of the absolute temperature; Ordinate—$d(E_g-E_x)/dT$ eV (°K)$^{-1}$ (×10^6); Abscissas—temperature °K. (b) Integrated change in E_g-E_x, electron-phonon interaction term only, plotted against the reciprocal temperature; Activation energies: $(\hbar\omega)_\alpha=0.127\pm0.04$ eV; $(\hbar\omega)_\beta=0.096\pm0.003$ eV; $(\hbar\omega)_\gamma=0.041\pm0.006$ eV(?); $(\hbar\omega)_\delta=0.022\pm0.003$ eV; $(\hbar\omega)_\epsilon=0.012\pm0.004$ eV (?); Ordinate—$\Delta(E_g-E_x)$ eV (×10^4); Abscissa—$10^3/T$ (°K)$^{-1}$ (bottom).

The effect of intravalley scattering also appears in Fig. 8(b).[25] The appropriate phonon energies are selected at the subzone boundary[30] ($\sigma_{max}/2$) and once again the LA branch is expected to predominate. The ⟨100⟩ LA phonon energy is ~0.095 eV at $\sigma_{max}/2$ [Fig. 7(b)], in good agreement with $\hbar\omega_\beta$ from Fig. 8(b). $\hbar\omega_\gamma$ remains unexplained, since it is too small to be accounted for by TA intravalley scattering. $\hbar\omega_\gamma$ comes from the least well substantiated straight-line section of Fig. 8(b), however, and is probably an artifact.

Extrinsic Features of the Recombination Radiation

Besides being very specimen-dependent in intensity relative to band B, a general characteristic of the extrinsic bands is a very narrow half-bandwidth.[2] The observed half-bandwidths of the most prominent extrinsic features in the diamond spectra (C, D and X, Y) are largely due to the instrumental resolution. This fact, together with the position of these bands just below band A suggests that the extrinsic bands may be due to the recombination of excitons which are bound to impurity or defect centers.[2,7] Two distinct centers are required, since the C, D bands were only detected for the type-IIb specimens, whose spectra show no trace of the X, Y bands exhibited by diamonds of other types. This makes it likely that the relevant IIb impurity is the unionized acceptor center, which has been attributed to substitutional aluminum. The dependence of the $C+D$ intensity on E_e given in Table I may then be due to a decrease in the acceptor concentration with penetration depth. A component corresponding in position with C, D below the first phonon emission threshold has been observed in the edge absorption and edge luminescence excitation spectra.[13,15] The $C-D$ separation is greater than the B_1-B_2 separation, but the difference, 0.004 eV, is not very significant. The double impurity band may therefore arise through coupling with each of the two main band B components, since the intensity ratio C/D is comparable with that of B_1/B_2. The binding energy E_d of the exciton to the impurity center is given by the displacement of C, D below the B_1 and B_2 thresholds (mean value 0.056 eV). The rapid temperature dependence of the intensity of the impurity lines is consistent with this interpretation[2] but no quantitative measurements of this variation were made. E_d is about 15% of the acceptor binding energy, which is consistent with the deduction that the electron effective mass is significantly less than the hole effective mass in diamond.[2,15]

Bands X, Y are respectively 0.009 eV below the thresholds of B_1 and B_2, but the intensity ratio X/Y is only about half of that attributed to B_1/B_2. These bands are observed in some of the nonsemiconducting diamonds, but the nature of the relevant impurity or defect is unknown. E_d is likely to be proportional to the ionization energy of the shallow donor or acceptor center[2] and these results therefore suggest that the ionization energy of the unknown center may be only ~0.06 eV (the value for the aluminium acceptor is ~0.37 eV). This low value is consistent with the expected ionization energy of the donor center in diamond according to the electron effective mass estimated from the exciton binding energy.[15] Bulk n-type thermally stimulated conductivity has yet to be observed in diamond, however, although it is known that electrons and holes can have comparable mobilities relatively perfect diamond.

Extrinsic emission bands are also expected to appear at E_d below E_g-E_x. Bands C', D' cannot be explained in this way since they do not occur at the predicted position and their intensity is not strictly proportional to that of bands C, D. No evidence was found for extrinsic bands near E_g-E_x associated with bands X, Y, even though X, Y sometimes dominated the recombination spectrum (Fig. 1). Only *one* band is expected for "no-phonon" extrinsic recombination. Haynes[31] has recently found that the strength of the "non-phonon" compared to the "with-phonon" band involving exciton recombination at shallow donors and acceptors in silicon is small for centers with small ionization energies, and therefore small E_d values. These centers are generally connected with light impurity elements. The present results are also consistent with this correlation.

[30] F. J. Blatt, Solid State Phys. 4, 199 (1956).

[31] J. R. Haynes (private communication).

TABLE II. Energies and classification of recombination emission bands from diamond.[a]

Intrinsic		Extrinsic	
Band and threshold energy (eV)	Classification	Band and peak energy (eV)	Classification
A[b]; 5.325±0.002	Type α, $E_g-E_x-\hbar\omega_1$ (5.325 eV)	C', 5.375±0.002	?
B_1[b]; 5.276±0.001	Type α, $E_g-E_x-\hbar\omega_2$ (5.276 eV)	D', 5.361±0.002	?
B_2[b]; 5.268±0.001	Type α, $E_g-E_x-\hbar\omega_3$ (5.268 eV)	X, 5.267±0.001	Type γ, $E_g-E_x-\hbar\omega_2$ (5.267 eV)$-E_{d_2}$
B_3[b]; 5.245±0.002	Type β, $E_g-E_x-\hbar\omega_3$ (5.245 eV)$-\hbar\omega_4$	Y, 5.259±0.001	Type γ, $E_g-E_x-\hbar\omega_3$ (5.259 eV)$-E_{d_2}$
E[b]; 5.133±0.003	Type β, $E_g-E_x-\hbar\omega_3$ (5.134 eV)$-\hbar\omega_2$	C, 5.222±0.001	Type γ, $E_g-E_x-\hbar\omega_2$ (5.220 eV)$-E_{d_1}$
F[b]; 5.098±0.002	Type α? $E_g-E_x-\hbar\omega_3$ (5.103 eV)$-\hbar\omega_R$	D, 5.210±0.001	Type γ, $E_g-E_x-\hbar\omega_3$ (5.212 eV)$-E_{d_1}$
K[c]; 4.987±0.003	Type α? $E_g-E_x-\hbar\omega_1$ (5.495 eV)$-2\hbar\omega_R$	G, 5.090±0.003	?
L[c]; 4.922±0.006	Type α? $E_g-E_x-\hbar\omega_3$ (4.938 eV)$-2\hbar\omega_R$	H, 5.076±0.002	Type γ? $E_g-E_x-\hbar\omega_2$ (5.078 eV)$-\hbar\omega_3-E_{d_1}$
		I, 5.059±0.002	?
		J, 5.034±0.003	?

[a] Classification types: α—intrinsic exciton annihilation with phonon emission; β—intrinsic exciton annihilation involving intervalley scattering; γ—extrinsic exciton annihilation occurring at defect or impurity. Symbols: E_g—indirect energy gap; $\hbar\omega_i$—phonon energy—see text; E_x—exciton binding energy; $\hbar\omega_R$—Raman energy; E_{d_1}—binding energy of exciton to C, D defect-substitutional aluminum (magnitude 0.056 eV); E_{d_2}—binding energy of exciton to X, Y defect-unknown nature (magnitude 0.009 eV).
[b] Threshold energies of these bands obtained from extrapolation of fitted Maxwell-Boltzmann curves.
[c] Threshold energies of these bands obtained assuming difference between apparent threshold and M.B. fit is the same as for band F.

CONCLUSION

A comprehensive list of the emission bands is given in Table II together with a review of the interpretation scheme proposed above. The most serious shortcomings in the present scheme are encountered in dealing with the extrinsic bands (bands near to E_g-E_x). As previously noted, some of the band with lower values of E_i which are listed as intrinsic in Table II may have been enhanced by the effects of suitable defects.

ACKNOWLEDGMENTS

One of us (I.H.J.) is grateful to the Department of Industrial and Scientific Research for the provision of a maintenance grant during the course of this work. Thanks are due to A. Benfield, H. Lemke, and D. Risley for extensive technical assistance and advice. We are indebted to Dr. J. R. Haynes for communicating some unpublished results on silicon and for a stimulating discussion of this work.

PHYSICAL REVIEW VOLUME 133, NUMBER 6A 16 MARCH 1964

Piezoresistive Properties of Heavily Doped *n*-Type Silicon*

O. N. TUFTE AND E. L. STELZER
Honeywell Research Center, Hopkins, Minnesota
(Received 16 October 1963)

The piezoresistance effect has been studied in *n*-type silicon over the impurity concentration range from approximately 1×10^{15} to 1×10^{20} cm^{-3}. From the analysis of the results, it is concluded that for Fermi energies up to 0.08 eV above the band edge, the total number of states below the Fermi level is correctly given by assuming that the band is parabolic with a density-of-states effective mass equal to that found in pure silicon. The qualitative dependence of the mobility anisotropy on impurity concentration and temperature is determined from the piezoresistance results. From the temperature dependence of the coefficient π_{11}, it is concluded that the deformation potential in *n*-type silicon increases by approximately 25% between 77 and 300°K. Finally, the π_{44} coefficient is found to increase with increasing impurity concentration at the highest concentrations. This behavior is attributed to the Fermi level approaching the energy of the conduction band at the [100] zone boundary in silicon having an electron concentration of the order of 1×10^{20} cm^{-3}.

I. INTRODUCTION

DURING the past decade, the properties of relatively pure *n*-type silicon have been extensively investigated to the point that it is today one of the best understood semiconductor materials. Cyclotron resonance, optical and galvanomagnetic measurements have clearly defined the energy-band structure near the band edge and have led to a quantitative understanding of the scattering mechanisms in lightly doped silicon. However, much less attention has been given to the properties of heavily doped silicon, where the term heavily doped here refers to doping levels between the concentration at which the impurity activation energy

* A preliminary account of this work was presented at the American Physical Society Meeting, March 1963, at St. Louis, Missouri.